RGNZ/MGPB

The performance analysis of the post-mission web-based static and kinematic PPP-AR service

Rudarsko-geološko-naftni zbornik
(The Mining-Geology-Petroleum Engineering Bulletin)
UDC: 528.4
DOI: 10.17794/rgn.2023.4.9

Original scientific paper

Bilal Mutlu[1]; Serdar Erol[2]; Reha Metin Alkan[3]

[1] Istanbul Technical University, Department of Geomatics Engineering - Türkiye, ORCID 0000-0002-9763-0345
[2] Istanbul Technical University, Department of Geomatics Engineering - Türkiye, ORCID 0000-0002-7100-8267
[3] Istanbul Technical University, Department of Geomatics Engineering - Türkiye, ORCID 0000-0002-1981-9783

Abstract

The use of the Precise Point Positioning (PPP) technique has become very advantageous with the development of GNSS positioning technology. It is possible to get highly accurate position information without the need of any reference station data using the PPP technique. However, there are various factors that affect the accuracy of PPP solutions, including the initial phase ambiguity solution type, which can be fixed or float, atmospheric effects, observation length, used satellite systems, and used precise products. The Canadian Spatial Reference System-Precise Point Positioning (CSRS-PPP) service, one of the online PPP services, was updated on October 20th, 2020, and upgraded to version 3, capable of the Ambiguity-Fixed (PPP-AR) solution. Prior to this date, the service had offered the Ambiguity-Float (PPP-Float) solution. In this study, it is aimed to investigate the effect of using different satellite systems (GPS, GPS&GLONASS), length of observation time, static/kinematic processing modes, and initial phase ambiguity solution types on PPP accuracy. The daily observation data of ANKR, ISTA, IZMI, MERS, and KRS1 IGS GNSS stations located within the borders of Türkiye, divided into different sub-sessions (1-hour, 2-hours, 4-hours, 8-hours, and 12-hours) were processed using CSRS-PPP web-based service as PPP-Float before the update and PPP-AR after the update. As a result of the comparison, the combined use of GPS & GLONASS satellite systems instead of using GPS satellites alone has increased horizontal and vertical accuracy in both static/kinematic PPP-Float and PPP-AR solutions. Considering the static solutions, horizontal and vertical position accuracies increase as the observation time increases in both ambiguity solution methods using different constellations. In the case of comparison of the ambiguity solution methods, it was found that the PPP-AR approach offered higher accuracy than the PPP-Float in all solution cases.

Keywords:
GPS; GLONASS; PPP-AR; PPP-Float; CSRS-PPP

1. Introduction

Precise Point Positioning (PPP) is an absolute positioning technique that enables the determination of a point position with up to centimeter-level or even more accuracy with a single GNSS receiver using precise products of GNSS satellites. With the development of technology and the ease of access to it worldwide, positioning systems and methods have also developed. The most important of these developments is the diversification of positioning constellations and the increased number of active satellites. In parallel with these developments, IGS started the Multi-GNSS Experiment (MGEX) project to get the precise multi-GNSS products in the same datum and time system. There are various studies that have been done to reveal the importance of the PPP technique in the positioning community, especially since 2000 (**Choy et al., 2017; Dawidowicz, 2020; DeSanto et al., 2019; Erol et al., 2020; Facio and Berber, 2020; Héroux and Kouba, 2001; Katsigianni et al., 2019; Kiliszek et al., 2018; Pırtı et al., 2023; Topal and Akpinar, 2022**).

Many academic and commercial desktop software are available for processing GNSS data using the PPP technique in post-mission and real-time modes. Besides, there are several web-based post-mission PPP services provided by different organizations. One of the major benefits of online GNSS PPP services is that they are free, precise, and user-friendly. Web-based services do not necessitate any extra software or particular features on the computer. The online PPP services need only a single GNSS receiver data file and choosing some basic options, such as data processing modes (static/kinematic), antenna type of receiver, and reference coordinate system (**Bahadur and Üstün, 2014**). After uploading the data, the services start to process and send the results to users in various formats after a short period of time, depending on the size of the collected GNSS data,

Corresponding author: Bilal Mutlu
e-mail addres: mutlubil@itu.edu.tr

internet speed, and server traffic. These results contain not only PPP coordinates, but also additional information (processing parameters, accuracy measures, number of satellites, satellite visibility, zenith tropospheric delay, dilution of precision) that will enable the interpretation of the solutions, enriching them with graphs and tables. While some services only accept GPS observations, many of them support other satellite constellations in their calculations and produce a multi-GNSS PPP solution. On the other hand, one of the most important parts of the PPP technique is the solution type of initial phase ambiguities, which can be fixed or float. A limited number of services provide PPP-AR solutions, while most of them solve ambiguities as a float. Fixing the ambiguities, also called PPP with Ambiguity Resolution (PPP-AR), gives more accurate solutions than ambiguity float (PPP-Float) solutions. There are different approaches to performing ambiguity fixed solutions, such as the "Decoupled Clock Model" (**Collins, 2008; Collins et al., 2010**), "Single-Difference Between Satellites Method" (**Ge et al., 2008**), and the "Integer Phase Clock Model" (**Laurichesse et al., 2009**).

The Canadian Spatial Reference System - Precise Point Positioning (CSRS-PPP) service, operated by National Resources Canada (NRCan), is one of the most popularly used web-based online PPP services. CSRS-PPP has provided PPP service over the web since 2003 (**Klatt and Johnson, 2017**). Thanks to the update on October 20th, 2020, CSRS-PPP started to produce the Ambiguity-Fixed (PPP-AR) solution for GPS satellites. This PPP-AR feature, which comes with this update, is provided according to the Decoupled Clock Model first defined by Collins in 2008 (**Collins, 2008**).

As an alternative to the CSRS-PPP service, Trimble Company also has a web-based online post-processing PPP service called CenterPoint RTX (Real Time eXtended), which produces the PPP-AR solution. In addition to this post-processing PPP (RTX-PP) service offered free of charge, the company also offers commercial real-time PPP (RT-PPP) service with the same name. Both post-processing and real-time services support Multi-GNSS (GPS, GLONASS, Galileo, BeiDou, QZSS) constellations and use the same products that are produced in real-time (**Doucet et al., 2012**). According to the official Trimble RTX webpage, RTX-PP service has an accuracy level of 2 cm or better for horizontal and 6 cm for vertical for the minimum 1-hour static observation period. However, as long as the static observation time increases, horizontal and vertical accuracies reach to 1 cm and 3 cm, respectively (**URL-1**). Although it has been stated that this service provides a solution with the PPP-AR approach, in general, worse results have been obtained than with the CSRS-PPP-Float (**Mutlu et al., 2020**).

In the scope of the study, an accuracy comparison was performed for CSRS-PPP-Float and CSRS-PPP-AR (PPP-Fixed) solutions. In order to test the positioning performance of the updated CSRS-PPP online service, daily observations obtained from several International GNSS Service (IGS) stations located in Türkiye, namely ISTA, ANKR, IZMI, MERS, and KRS1, dated January 1st, 2020, were used. The daily observations were split into sub-sessions as 1, 2, 4, 8, and 12 hourly data groups, and each observation group was processed according to GPS-only (G) and GPS&GLONASS (GR) constellations. The version 3 update of the CSRS-PPP service in October 2020, provided an opportunity to compare the accuracy performances of PPP-AR against PPP-Float solutions. Within the scope of this study, all data were processed as PPP-Float before the update and as PPP-AR afterward. The static and kinematic PPP-AR accuracy performance of the CSRS-PPP online service was tested according to different constellations (G and GR) and different observation durations and compared with the PPP-Float solutions of the service.

2. Precise Point Positioning (PPP)

The PPP technique was originally proposed by Anderle in 1976 (**Anderle, 1976**) and subsequently refined by Zumberge et al. in 1997 (**Zumberge et al., 1997**). Since then, it has been widely utilized in various static/kinematic, scientific/practical applications as real-time/post-processed, across the world.

The fact that users can collect data with a single GNSS receiver to determine the position information provides freedom of operation, makes the technique easy to apply, and significantly reduces the cost of measurement. Despite these important advantages, the technique also has some shortcomings, the most important of which is a convergence time of 20-30 minutes or more required to achieve accuracy in centimeters. This situation makes the technique difficult or even restricted to be used in real-time applications. However, convergence time is not a major obstacle for post-mission PPP processing because, in this case, the data is processed forward and backward and combined optimally. PPP ambiguity fixed solutions contribute to the shortening of the convergence time and provide higher accuracy and reliability than the ambiguity float solution (**Bisnath and Collins, 2012**). The code and phase observation equations for the multi-GNSS PPP model are given below (**Hofmann-Wellenhof et al., 2007; Xiao, 2022; Xu and Xu, 2007**):

$$P_{i,r}^{S} = \rho_r^S + cdt^r - cdt^S + T_r^S + \frac{f_1^2}{f_i^2} I_{r,1}^S + b_{P_i}^r - b_{P_i}^S + \varepsilon\left(P_{i,r}^S\right)$$

$$\Phi_{i,r}^{S} = \rho_r^S + cdt^r - cdt^S + T_r^S - \frac{f_1^2}{f_i^2} I_{r,1}^S - \lambda_i N_i + b_{\Phi_i}^r - b_{\Phi_i}^S + \varepsilon\left(\Phi_{i,r}^S\right) \quad (1)$$

In the equations, r and i represent the receiver and signal frequency, respectively, and S shows the GNSS type (G: GPS, R: GLONASS, etc.). Also, $P_{i,r}^S$ is code observation (m), $\Phi_{i,r}^S$ is phase observation (m), ρ_r^S is the geometric distance between satellites and receiver (m), c is the speed of light (m/s), dt^r is receiver clock error (s), dt^s is satellite clock error (s), T_r^S is tropospheric delay(m), f_i is the frequency of related signal (Hz), $I_{r,1}^S$ is the slant ionospheric delay on the first carrier frequency (m), $b_{P_i}^r$

and $b^S_{P_i}$ are the code hardware delays (bias) of receiver and satellite (m), N_i is phase ambiguity, λ_i is wavelength of related signal frequency (m), $b^r_{\Phi_i}$ and $b^S_{\Phi_i}$ are receiver and satellite phase hardware delays (bias) in meter and ε represents other non-modelled errors including multipath error (m). But, to eliminate first-order ionospheric delay, iono-free (IF) linear combinations of phase and code observation equations are produced with the help of a combination of dual frequencies as given below (**Zumberge et al., 1997**).

$$\alpha_{IF} = \frac{f_1^2}{\left(f_1^2 - f_2^2\right)}; \beta_{IF} = \frac{-f_2^2}{\left(f_1^2 - f_2^2\right)}$$

$$P^S_{IF,r} = \alpha_{IF} P^S_{1,r} + \beta_{IF} P^S_{2,r}$$

$$\Phi^S_{IF,r} = \alpha_{IF} \Phi^S_{1,r} + \beta_{IF} \Phi^S_{2,r}$$

$$\lambda_{IF} = \frac{2cf_0}{\left(f_1^2 - f_2^2\right)} \tag{2}$$

The satellite iono-free code and phase biases ($b^S_{P_{IF}}$ and $b^S_{\Phi_{IF}}$) are included in satellite clock errors ($cdt^S_{P_{IF}}$ and $cdt^S_{\Phi_{IF}}$) according to the combination principle. In addition, the receiver clock errors ($cdt^r_{P_{IF}}$ and $cdt^r_{\Phi_{IF}}$) are estimated as including an iono-free combination of the receiver code and phase biases ($b^r_{P_{IF}}$ and $b^r_{\Phi_{IF}}$). So that, if clock errors and related biases are assigned to single variables, the equations will be as follows:

$$P^S_{IF,r} = \rho^S_r + cdt^r_{P_{IF}} - cdt^S_{P_{IF}} + T^S_r + \varepsilon\left(P^S_{IF,r}\right)$$

$$\Phi^S_{IF,r} = \rho^S_r + cdt^r_{\Phi_{IF}} - cdt^S_{\Phi_{IF}} + T^S_r - \lambda_{IF}\left(17N_1 + 60N_{WL}\right) + \varepsilon\left(\Phi^S_{IF,r}\right)$$

$$\begin{cases} cdt^r_{P_{IF}} = cdt^r + b^r_{P_{IF}};\ cdt^S_{P_{IF}} = cdt^S + b^S_{P_{IF}} \\ cdt^r_{\Phi_{IF}} = cdt^r + b^r_{\Phi_{IF}};\ cdt^S_{\Phi_{IF}} = cdt^S + b^S_{\Phi_{IF}} \end{cases}$$

$$\begin{cases} b^r_{P_{IF}} = \alpha_{IF} b^r_{P_1} + \beta_{IF} b^r_{P_2};\ b^S_{P_{IF}} = \alpha_{IF} b^S_{P_1} + \beta_{IF} b^S_{P_2} \\ b^S_{\Phi_{IF}} = \alpha_{IF} b^S_{\Phi_1} + \beta_{IF} b^r_{\Phi_2};\ b^S_{\Phi_{IF}} = \alpha_{IF} b^S_{\Phi_1} + \beta_{IF} b^S_{\Phi_2} \end{cases} \tag{3}$$

Equations that need to be obtained to produce the ambiguity fixed solution are the Wide-Lane phase equation, the Narrow-Lane pseudo-range equation, and also the Hatch-Melbourne-Wübbena (HMW) function, which eliminates atmospheric delays, geometric distance, satellite and receiver clock errors (**Hatch, 1983; Melbourne, 1985; Wübbena, 1985**).

The Wide-Lane phase combination ($\Phi^S_{r,WL}$) can be written as:

$$\alpha_{WL} = \frac{f_1}{\left(f_1 - f_2\right)}; \beta_{WL} = \frac{-f_2}{\left(f_1 - f_2\right)}$$

$$\Phi^S_{r,WL} = \alpha_{WL} \Phi^S_{1,r} + \beta_{WL} \Phi^S_{2,r}$$

$$N_{WL} = N_1 - N_2$$

$$\Phi^S_{r,WL} = \rho^S_r + cdt^r - cdt^S + T^S_r + \frac{f_1^2}{f_2^2} I^S_{r,1} + \left(\alpha_{WL} b^r_{\Phi_1} + \beta_{WL} b^r_{\Phi 2}\right) -$$

$$\left(\alpha_{WL} b^S_{\Phi_1} + \beta_{WL} b^S_{\Phi 2}\right) - \lambda_{WL} N_{WL} + \varepsilon\left(\Phi^S_{r,WL}\right) \tag{4}$$

The Narrow-Lane code combination ($P^S_{r,NL}$) can be written as:

$$\alpha_{NL} = \frac{f_1}{\left(f_1 + f_2\right)}; \beta_{NL} = \frac{f_2}{\left(f_1 + f_2\right)}$$

$$P^S_{r,NL} = \alpha_{NL} P^S_{1,r} + \beta_{NL} P^S_{2,r}$$

$$P^S_{r,NL} = \rho^S_r + cdt^r - cdt^S + T^S_r + \frac{f_1^2}{f_2^2} I^S_{r,1} +$$

$$\left(\alpha_{NL} b^r_{P_1} + \beta_{NL} b^r_{P_2}\right) - \left(\alpha_{NL} b^S_{P_1} + \beta_{NL} b^S_{P_2}\right) + \varepsilon\left(P^S_{r,NL}\right) \tag{5}$$

HMW function can be obtained with the help of $\Phi^S_{r,WL}$ and $P^S_{r,NL}$ functions as follows:

$$A_{HMW} = \Phi^S_{r,WL} - P^S_{r,NL}$$

$$A_{HMW} = b^r_{A_{HMW}} - b^S_{A_{HMW}} - \lambda_{WL} N_{WL} + \varepsilon\left(A^S_{HMW,r}\right)$$

$$\begin{cases} b^r_{A_{HMW}} = \left(\alpha_{WL} b^r_{\Phi_1} + \beta_{WL} b^r_{\Phi_2}\right) - \left(\alpha_{NL} b^r_{P_1} + \beta_{NL} b^r_{P_2}\right) \\ b^S_{A_{HMW}} = \left(\alpha_{WL} b^S_{\Phi_1} + \beta_{WL} b^S_{\Phi_2}\right) - \left(\alpha_{NL} b^S_{P_1} + \beta_{NL} b^S_{P_2}\right) \end{cases} \tag{6}$$

So far, general PPP GNSS observations and linear functions have been explained, and from here on, the Decoupled Clock Model (DCM) method has been elaborated since the CSRS-PPP web-based online service produces the solution according to the DCM method. DCM, which contains separate satellite clocks for code and phase observations, was developed by **Collins et al. (2010)**. For the DCM solution, 3 different equations derived above and given below are used.

$$P^S_{IF,r} = \rho^S_r + cdt^r_{P_{IF}} - cdt^S_{P_{IF}} + T^S_r + \varepsilon\left(P^S_{IF,r}\right)$$

$$\Phi^S_{IF,r} = \rho^S_r + cdt^r_{\Phi_{IF}} - cdt^S_{\Phi_{IF}} + T^S_r - \lambda_{IF}\left(17N_1 + 60N_{WL}\right) + \varepsilon\left(\Phi^S_{IF,r}\right)$$

$$A_{HMW} = \Phi^S_{r,WL} - P^S_{r,WL} = b^r_{A_{HMW}} - b^S_{A_{HMW}} - \lambda_{WL} N_{WL} + \varepsilon\left(A^S_{HMW,r}\right) \tag{7}$$

In the solutions to be made according to this model, the parameters are divided into two as satellite and receiver DCM parameters ($cdt^S_{P_{IF}}$, $cdt^S_{\Phi_{IF}}$, $b^S_{A_{HMW}}$) and ($cdt^r_{P_{IF}}$, $cdt^r_{\Phi_{IF}}$, $b^r_{A_{HMW}}$), respectively. Suppose the solution is to be implemented for one station. In that case, the unknowns are, respectively 3 coordinates, 3 receiver DCM parameters, 3n (n: number of satellites) satellite DCM parameters, 1 tropospheric delay, and 2(n-1) N_{WL} and N_1 ambiguities. Since the number of unknown variables is high, satellite DCM parameters should be calculated with the help of network solutions.

The satellite DCM parameters ($cdt^S_{P_{IF}}$, $cdt^S_{\Phi_{IF}}$, $b^S_{A_{HMW}}$) obtained from the network solution are required for the PPP-AR solution with a single receiver by using DCM. By knowing the satellite DCM parameters and determining the ambiguity datum, the unknown parameters become estimable for the DCM equations. So, the integer N_{WL} and N_1 ambiguities can be directly estimated in the functional model. Suppose the satellite DCM parameters and the ambiguity datum are available. In that case, the unknown parameters become 3 coordinates, 3 receiver

DCM parameters, 1 tropospheric delay, and 2(n-1) ambiguities (N_{WL} and N_1) in DCM. In this case, the degree of freedom can be calculated as n-5, so a minimum of 5 satellites must be observed in order to perform the PPP-AR according to DCM (**Shi, 2012; Shi and Gao, 2014**).

Unlike the "Decoupled Clock Model", which isolates receiver/satellite code/phase biases from integer ambiguities, the "Single-Difference between Satellites Method" first estimates the real-valued IF ambiguity and then recovers the integer property by applying satellite fractional-cycle bias (FCB) corrections (**Shi and Gao, 2014**). The integer property of PPP ambiguities in this method can be recovered with the satellite wide-lane and N_1 FCB corrections. In the "Integer Phase Clock Model", the wide-lane satellite bias corrections are used to resolve the integer wide-lane ambiguity, whereas the integer N_1 ambiguity is directly estimated (**Laurichesse et al., 2009; Loyer et al., 2012**).

3. The Canadian Spatial Reference System-PPP (CSRS-PPP)

The Canadian Spatial Reference System Precise Point Positioning (CSRS-PPP) service provided by Natural Resources Canada (NRCan) has been offering free of charge PPP solutions to all scientific and commercial users around the world since 2003 (**Klatt and Johnson, 2017**). CSRS-PPP has reduced the complex sequence operations of GNSS data processing to a form that users can easily perceive. It has been designed to provide users with a straightforward and efficient way to estimate the position even without theoretical knowledge of GNSS and PPP (**Klatt and Johnson, 2017**). Single or dual-frequency GNSS data can be used to produce static or kinematic PPP coordinates, and the users just need to upload an observation file (RINEX, *.zip, *.gzip, *.gz, *.z, *.YYo) to the website by selecting processing options such as reference frame (NAD83 or ITRF), processing mode (static or kinematic) and Ocean Tide Loading (OTL) file. After that, related solutions are sent to the stated valid e-mail addresses. During the process, the service uses GPS and GLONASS observation data, but it is planned to use all GNSS constellations and signals in the near future (**URL-2**). CSRS-PPP has provided solutions as PPP-Float until October 20th, 2020. After this date, the CSRS-PPP system upgraded to CSRS-PPP-Ambiguity Resolution (PPP-AR), and solutions were produced by fixing the GPS ambiguities based on the decoupled clock model (DCM) (**Banville et al., 2021**) for the data collected after January 1st, 2018. Thanks to the PPP-AR technique used by the new version of the CSRS-PPP service, the convergence time required to achieve centimeter accuracy has been reduced, and the accuracy of the east component improved by about 50% (**Atiz and Kalayci, 2021**). The CSRS-PPP service evaluated the GNSS data using the best precise satellite orbit and clock products (ultra-rapid, rapid, or final) that IGS/NRCan have produced at that time and calculated PPP coordinates as static or kinematic. IGS products, produced with the help of the worldwide IGS network of 515 stations, include orbit and clock information of satellites in high accuracy; this is the main advantage of CSRS-PPP because the most critical error sources of PPP are orbit and clock product quality. However, the new version of CSRS-PPP, which is CSRS-PPP-AR, uses precise satellite orbit and clock products that are ultra-rapid (DCU), rapid (DCR), and final (DCF) products produced by NRCan to perform ambiguity resolution. DCF products are a combination of the IGS final orbits file and the clock corrections data, which is produced by NRCan (**Banville, 2020**). CSRS-PPP processes the data of dual-frequency multi-GNSS (GPS and GLONASS) data obtained by static or kinematic observation and performs these calculations using SPARK (Simon's PPP with Ambiguity Resolution using a Kalman filter), an academic software.

4. Case Study

In this study, the static and kinematic positioning performance of the CSRS-PPP online service was investigated for different observation lengths, and GNSS constellations. Furthermore, the effect of ambiguity solution strategies, i.e. float and ambiguity-fix, on the PPP solution was also examined. Within this frame, the handled GNSS dataset was processed with the PPP-Float approach and once again, PPP-AR. In this way, the contribution of PPP-AR solutions over the float ones was assessed in terms of horizontal and vertical position accuracies. In the context of the study, the ISTA, ANKR, IZMI, MERS, and KRS1 reference stations from the IGS Network were used as a dataset. All stations are within Türkiye's boundaries, as shown in **Figure 1**.

In the study, the daily multi-GNSS data of the IGS reference stations on January 1st, 2020 (GPS Week: 2086 and GPS Day: 001) were used. The necessary observation files were downloaded from the IGS web page. It should be noted here that although multi-GNSS (GPS, GLONASS, Galileo, BeiDou, and SBAS) observations were collected at the selected reference stations, only GPS and GLONASS observations were considered since the CSRS-PPP service can provide GPS-only and GPS&GLONASS solutions. Thus, the daily RINEX files were formed into two categories as GPS-only and combined GPS&GLONASS observations using GFZRNX open-source software (**Nischan, 2016**) to investigate the contribution of the GLONASS system on PPP solutions. After that, how the observation period affects the accuracy of the PPP position was investigated. In order to investigate this, station observations were divided into different time sessions. The daily observation data on 1st day of 2020 for all used IGS stations were divided into shorter sessions as 1-hourly, 2-hourly, 4-hourly, 8-hourly, and 12-hourly with respect to satellite systems

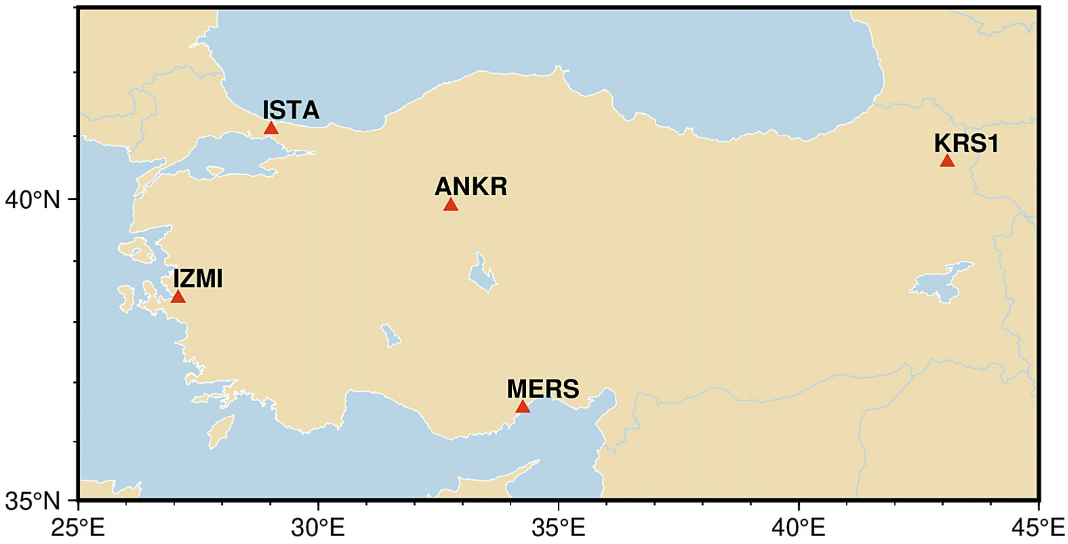

Figure 1: Location of IGS stations used in the study (created with **Wessel et al., 2019**).

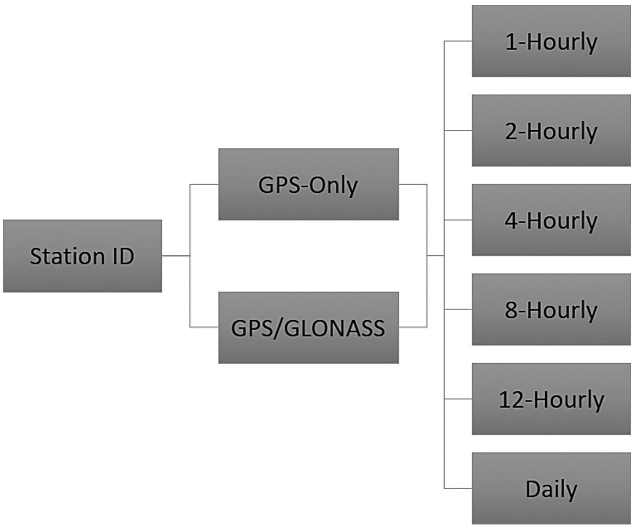

Figure 2: File hierarchy for RINEX files concerning constellations and observation durations.

as GPS-only (G) and a combination of GPS&GLONASS (GR) constellations, given in **Figure 2**. Totally, for both G and GR combination of 5 stations, 480 RINEX files [1 hourly (24 pieces), 2 hourly (12 pieces), 4 hourly (6 pieces), 8 hourly (3 pieces), 12 hourly (2 pieces), 24 hourly (1 piece)] were processed as both PPP-Float and PPP-AR using the CSRS online service.

Within the scope of this study, all RINEX data with different GNSS constellations and observation durations for all stations were processed as static and kinematic PPP-Float using CSRS-PPP v2.32.0 service before October 20th, 2020, and then the same processes were done again to get the PPP-AR solutions using CSRS-PPP v3.45.0 service, after October 20th, 2020. The processing options used in two different versions of the online service are given in the table below (see **Table 1**) (**Banville et al., 2021**).

After uploading all observation files to the CSRS-PPP service via its web-based interface, PPP results were sent to us via e-mail. The results contained PPP-derived current epoch ITRF coordinates, graphs, and some other reports. According to the results, there were some problems with the ANKR station observations. So, the results of the ANKR station were excluded from the study. Mean PDOP values and statistics for the number of satellites (NoS) for the stations were given in **Table 2**.

When **Table 2** was investigated, it was seen that with the use of GLONASS satellites together with GPS satellites, the mean number of satellites increased by 70% to reach approximately 20 satellites, and the PDOP value decreased by 30% to 1.3. The GPS and GLONASS L1 and L2 code multipath and SNR quality drawings obtained using BNC software (**URL-3**) were presented as skyplots in **Figure 3**.

When the skyplots were analysed, for the GNSS observations above the 7.5-degree elevation angle, it can be stated that the average of GPS and GLONASS L1 and L2 code multipath values at ISTA station was 30 cm. In addition, SNR values were on average 50 dbHz. Average multipath values for both frequencies at the IZMI station were 30 cm for GPS and 50 cm for GLONASS. The IZMI SNR values were 50 dbHz, similar to the ISTA station. But at the IZMI station, the SNR value of the GPS L2 frequency dropped to 30 dbHz at low elevation angles (between 7.5-30 degrees). Although the average multipath values in the KRS1 station were similar to the values in the IZMI station, there were some 1.5-2 meter multipath values above the 7.5-degree elevation angle because of the metal-clad roof that the station installed (see **Figure 4**). When the SNR values at the KRS1 station were investigated, it can be stated that the SNR values of the L2 measurements below the 30 degrees elevation angle for both satellite systems were below the 35 dbHz limit value (**Elango et al., 2017**). For the last station, MERS, the average of GPS and GLONASS L1 and L2 code multipath values were 20 cm, much lower than other stations' multipath values. The average SNR val-

Table 1: Processing options used by CSRS PPP-Float and PPP-AR versions.

CSRS-PPP Version	SPARK v2.32.0	SPARK v3.45.0
Processing Mode	Static, Kinematic	Static, Kinematic
GNSS Systems	GPS & GLONASS	GPS & GLONASS
Observations	Phase & Code	Phase & Code
Observation Interval (second)	30	30
Elevation Cut-off (degrees)	7.5	7.5
Frequency Used	L1 & L2	L1 & L2
Precise Satellite Products	IGS Final	NRCan Final
Phase Center Corrections	IGS (ATX)	IGS (ATX)
Reference Frame	ITRF14	ITRF14
Ionospheric Model	L3 (IF)	L3 (IF)
Mapping Function	VMF1	VMF1
Priori Tropospheric Model	Applied	Applied
Code biases	Applied	Applied
Phase biases	-	Applied
Phase wind-up	Modelled	Modelled
Solid Earth and Polar Tides	Modelled	Modelled
Marker (Station) Coordinates	Estimated	Estimated
Tropospheric Zenith Delay (TZD)	Estimated	Estimated
Receiver Clock Offset	Estimated	Estimated
Ambiguity Resolution	Float	Fixed

ues were similar for both satellite systems and their frequencies at 50 dbHz. As a result, the GNSS measurement quality at the KRS1 station was worse than the other stations, and the total number of cycle-slips at this station was quite high compared to other stations. The daily data for a number of cycle-slips obtained from the EUREF website of the KRS1 station for 2020 were given in **Figure 4**. According to **Figure 4**, cycle slips occurred in an average of 4000 of the observations obtained from GPS satellites and 8000 of the observations obtained from GLONASS satellites, which were monitored daily in the year 2020 at station KRS1.

5. Numerical Results

All GNSS RINEX observation files (384 in total without ANKR stations) containing GPS-only and GPS&GLONASS combination of all stations were processed as static in PPP-Float and PPP-AR mode using CSRS-PPP online service. Static solution coordinate values obtained for each station were compared with the known ITRF coordinates of the stations. By using GPS-only, GPS&GLONASS PPP-Float and PPP-AR static solutions and the known ITRF coordinates of the stations, horizontal (2D) and height (h) differences and RMS values were calculated for all observation durations (1h, 2h, 4h, 8h, 12h, 24h). Thus, online PPP-AR service performance according to different constellations and observation durations was tested and compared with PPP-Float solutions. **Figure 5** shows the static PPP-AR and PPP-Float horizontal and height differences for all stations at different observation durations and constellations. **Figure 6** shows the horizontal and height RMS values for all station static PPP solutions according to observation durations, ambiguity solution types, and constellations. It should be noted here that the CSRS-PPP service upgraded to version 3 only fixes the ambiguities of GPS satellites, not for GLONASS. In the rest of the text, the PPP-Float and PPP-AR solutions will be named Float and Fixed, respectively.

When **Figure 6** was investigated, it can be stated that the station with the lowest horizontal and vertical accuracy was KRS1, and the ISTA station had the highest accuracy for all solutions. The reason for the low position accuracy at the KRS1 station was probably related to the number of cycle-slips, multipath, and SNR values (see **Figures 3** and **4**). The different horizontal and vertical accuracies for all stations were related to changes in the quality of the observations depending on the receiver types, the troposphere conditions, and the environmental factors around the stations. When **Figure 6** was inspected, it can be stated that when R observations were combined with the G observations, horizontal and vertical accuracies provided improvement in both Float and Fixed solutions. However, Fixed solution accuracies for horizontal and vertical components significantly im-

Table 2: The statistics of the number of satellites (NoS) and mean PDOP values for the used IGS stations.

Station ID	GPS-Only				GPS&GLONASS			
	Min	Mean	Max	PDOP	Min	Mean	Max	PDOP
ANKR	5	6	8	8.4	9	13	17	2.1
ISTA	10	12	14	1.8	18	21	25	1.3
IZMI	10	12	14	1.8	17	19	22	1.4
KRS1	10	12	14	1.7	16	20	23	1.3
MERS	10	12	15	1.8	19	22	26	1.3

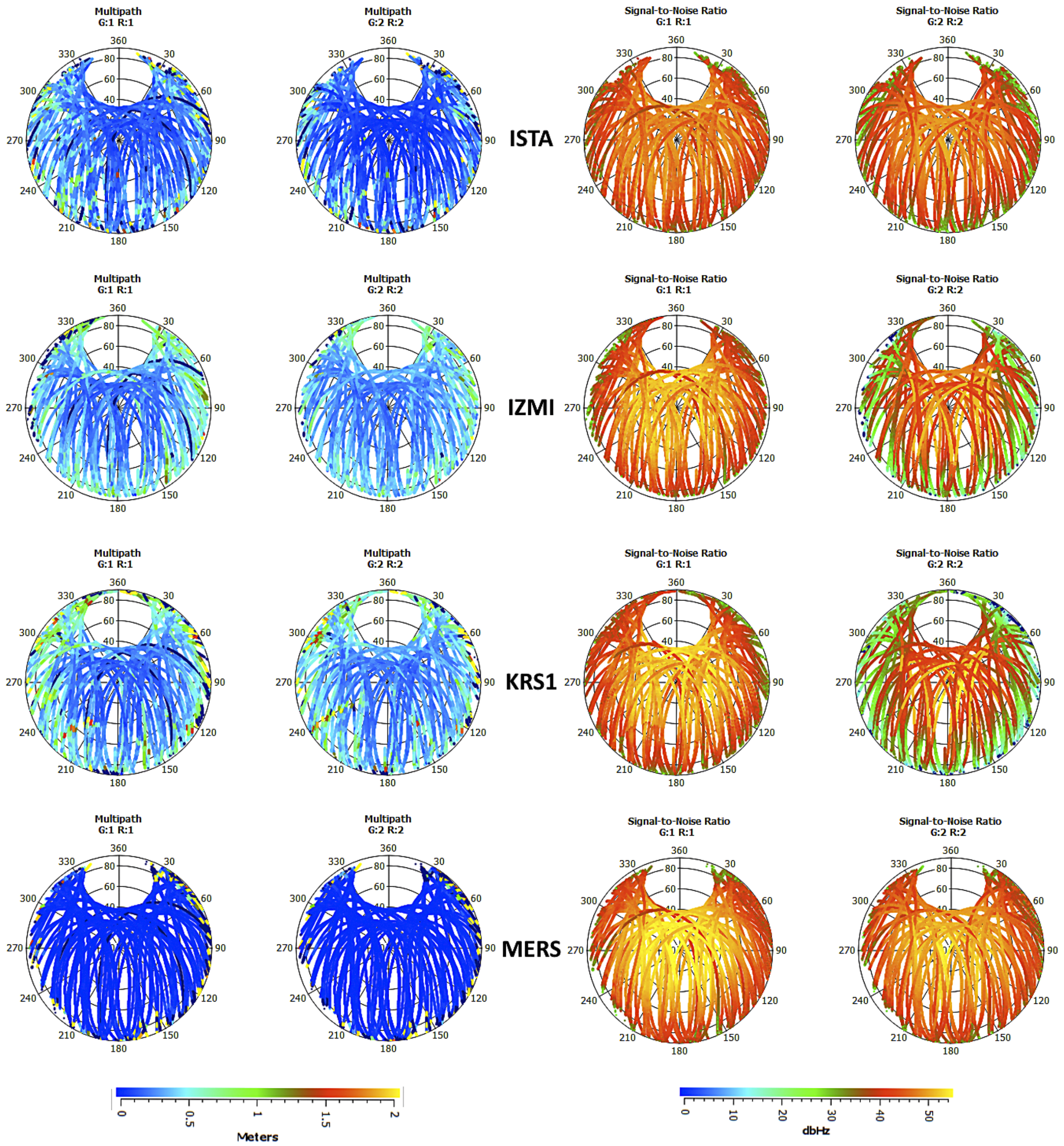

Figure 3: Multipath (left) and SNR (right) quality plots of GPS (G) and GLONASS (R) L1 and L2 observations for the IGS stations.

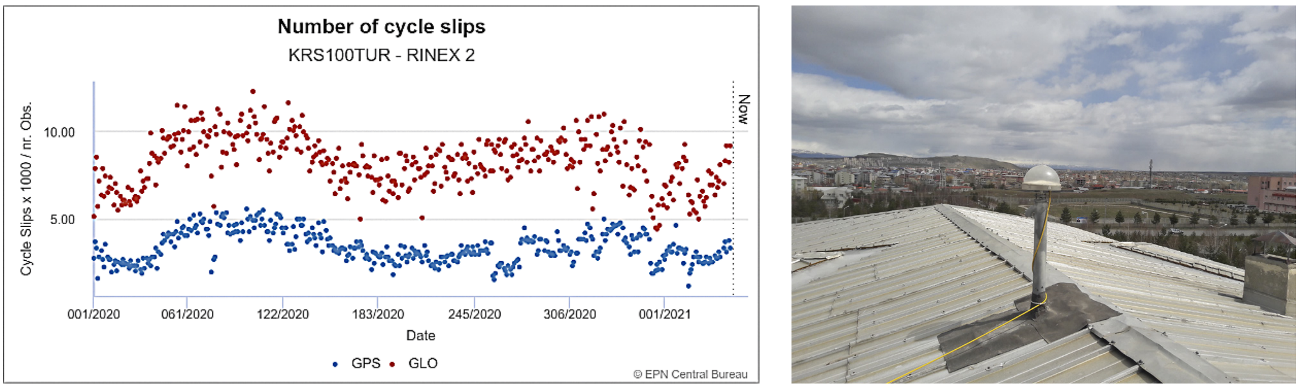

Figure 4: Number of cycle-slips at KRS1 station for GPS and GLONASS observations (*left*) and the location of the station on the metal-clad roof (*right*) (**URL-4**).

Figure 5: Static PPP solutions horizontal (2*D*) (top) and height (*h*) (bottom) differences for ISTA, IZMI, KRS1, and MERS stations according to constellations, ambiguity solution types, and duration times. (Each section of the figure has 1h, 2h, 4h, 8h, 12h, and 24h differences from top to bottom, respectively.)

proved compared to Float accuracies. As can be seen from the static PPP solutions of all stations, in order to improve the position accuracy, especially at 1-hour and 2-hour observation durations, the implementation of the PPP-AR solution was much more effective than adding GLONASS satellites to the solution (see **Figures 5** and **6**). When the AR ratios of static solutions were examined, it was obtained that the average AR rates of 1-hour solutions were over 90%, except for KRS1, and KRS1 was around 80%. Besides, if the observation periods of 4-hours or more, AR rates were determined over 95%. With the increase in observation duration, the accuracy of both Float and Fixed 2*D* and *h* solutions have increased for the G and GR observation groups. This result was valid for all stations. As a result of investigating the accuracies obtained from the static PPP solutions of the 1-hour observation groups of the ISTA station, the 2D horizontal accuracies for Float-G, Float-GR, Fixed-G,

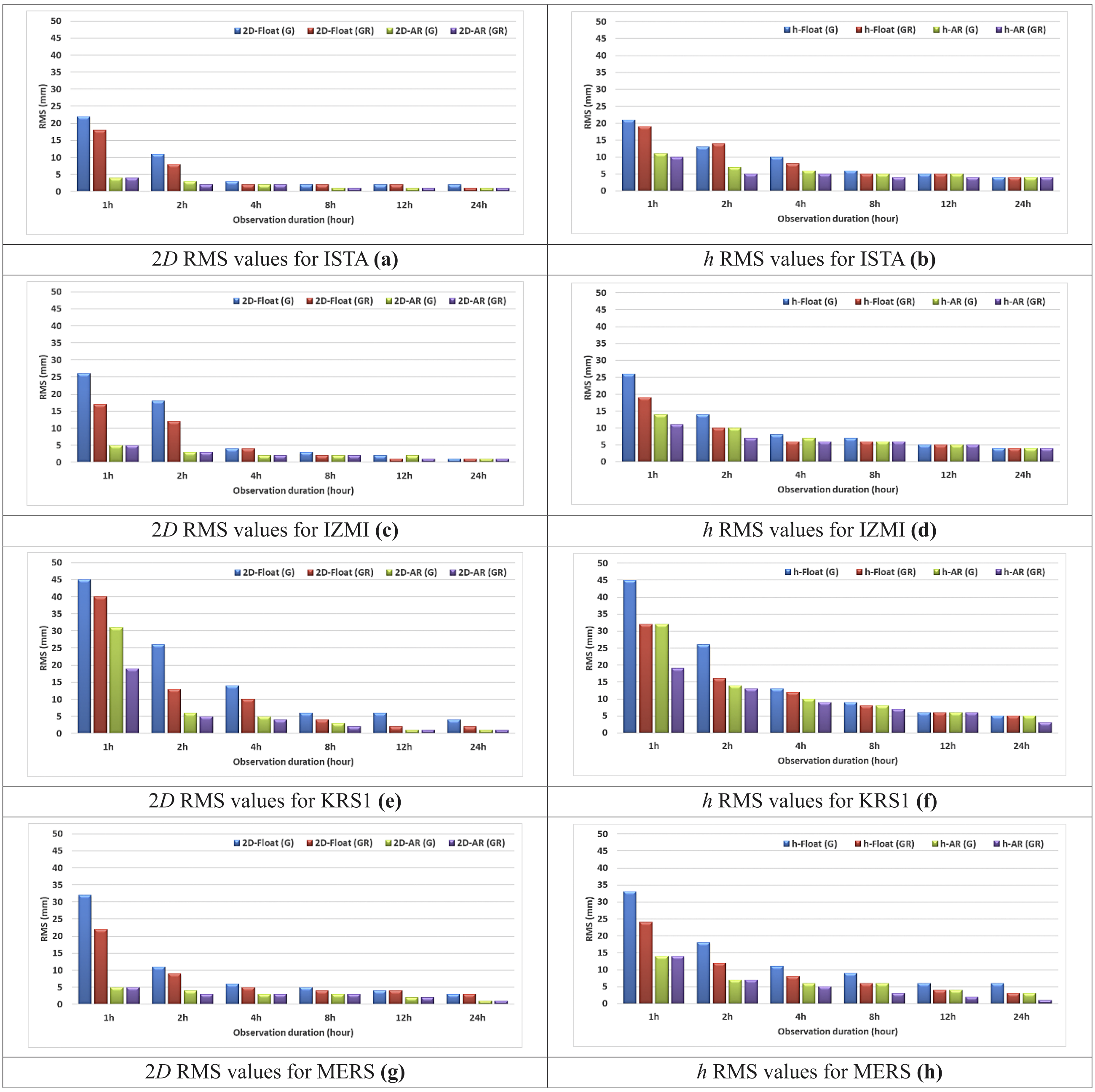

2*D* RMS values for ISTA **(a)** | *h* RMS values for ISTA **(b)** | 2*D* RMS values for IZMI **(c)** | *h* RMS values for IZMI **(d)** | 2*D* RMS values for KRS1 **(e)** | *h* RMS values for KRS1 **(f)** | 2*D* RMS values for MERS **(g)** | *h* RMS values for MERS **(h)**

Figure 6: Static PPP solutions horizontal (2*D*) (left) and height (*h*) (right) RMS values for ISTA, IZMI, KRS1, and MERS stations according to constellations, ambiguity solution types, and duration times.

and Fixed-GR were obtained as 22 mm, 18 mm, 4 mm, and 4 mm, respectively. Also, the height accuracies were found as 21 mm, 19 mm, 11 mm, and 10 mm in the same order. For the KRS1 station, 2D accuracies were found as 45 mm, 40 mm, 31 mm, and 19 mm; and height accuracies were found as 45 mm, 32 mm, 32 mm, and 19 mm, again in the same order. The 2D and height accuracies obtained in 2-hour measurements increased by approximately 50% compared to those obtained from 1-hour measurements. Except for the KRS1 station, Fixed solutions increased the accuracy by 50% in 1-hour and 2-hour solutions compared to the Float solutions both horizontally and vertically. For the observation durations longer than 2-hours, whether G, GR, Float, or Fixed solution, the horizontal position accuracy was better than 5 mm, the height accuracy was better than 1 cm, and the height RMS value decreased to 5 mm as the observation time increased.

In addition to static PPP solutions, each station's 24-hour data Float and Fixed kinematic PPP solutions were also compared with the known ITRF coordinates. The created time series and scatter plots for two solution strategies and two constellations were presented in **Figure 7** for all stations. Also, the easting, northing, and height RMS values were calculated from the obtained differences. The RMS values of the kinematic PPP solu-

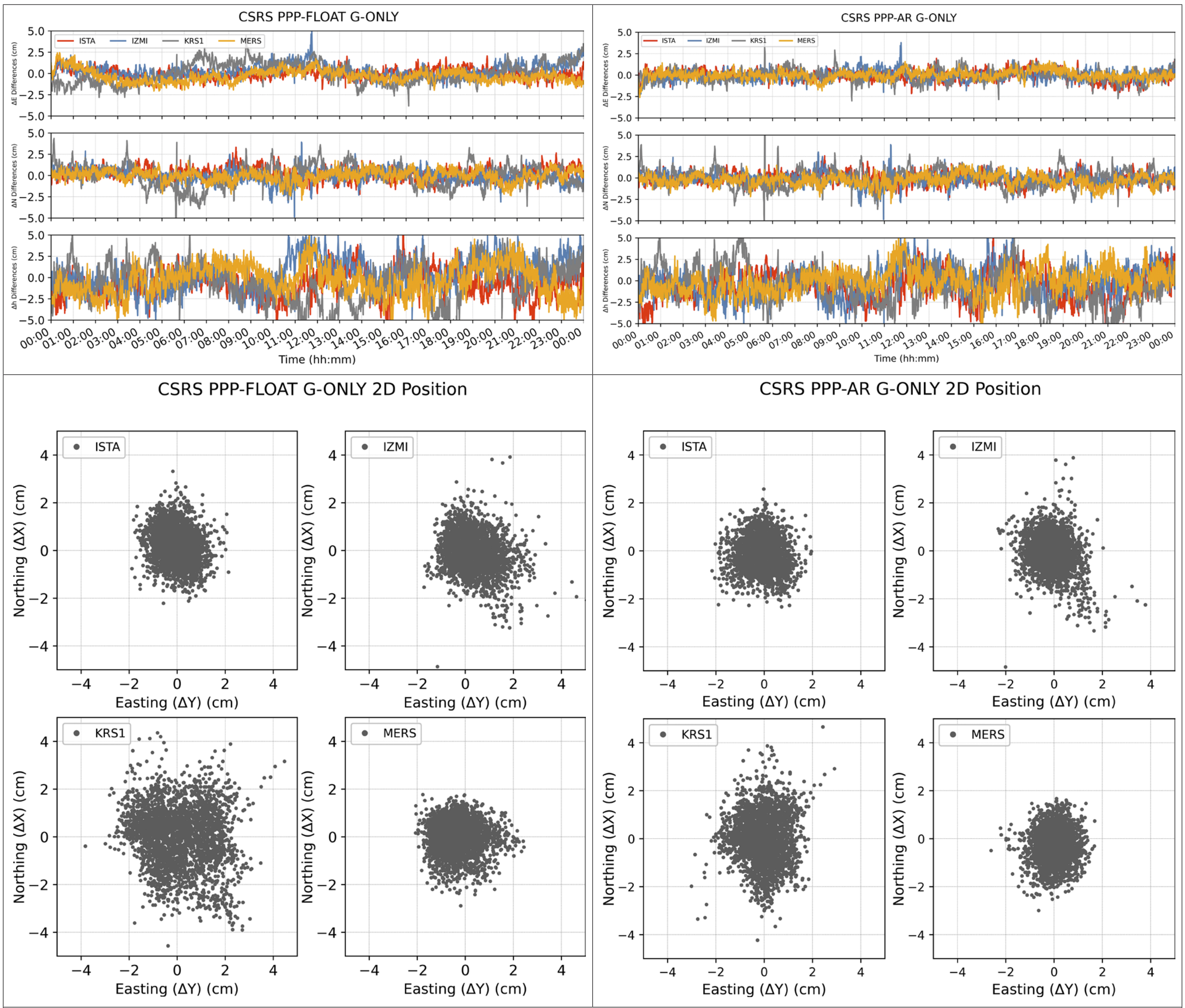

(a) G-only solutions

tions using both constellations and ambiguity solution strategies are given in **Figure 8** for all stations. According to **Figure 7** and **Figure 8** below for each station, both Float and Fixed kinematic PPP solutions have slightly increased the horizontal and height accuracy with the help of R observations. Similarly, in both G and GR kinematic PPP solutions, the Fixed solution has increased the horizontal position and height accuracy compared to the Float solution. When the AR ratios of kinematic solutions were examined, it was noticed that similar values were obtained with static solutions.

According to **Figure 8**, 2D horizontal position accuracies for each station were below 15 mm for Float-G and less than 10mm for Float-GR, Fixed-G, and Fixed-GR kinematic solutions. The height accuracies were obtained below 20 mm for Float-G and Fixed-G and around 15 mm for Float-GR and Fixed-GR, except for the KRS1 station.

6. Discussion and Conclusion

In this study, the static and kinematic accuracy improvement of the online PPP-AR solution service, an updated version of the CSRS-PPP service in October 2020, compared to the previous version of the service, which offered a PPP-Float solution, was investigated. Also, the performance of the CSRS-PPP-AR service was analyzed according to observation durations and the GNSS constellations used in the processing. For this purpose, daily observation data of 5 different IGS stations located into the border of Türkiye were used and processed with CSRS-PPP online post-processing service before and after the update as static and kinematic mode. First of all, the multi-GNSS daily RINEX data of the stations were prepared as two different daily data: GPS-only and GPS&GLONASS satellite systems. Then, each RINEX data group was divided into the sub-data groups into 1-hours, 2-hours, 4-hours, 8-hours, and

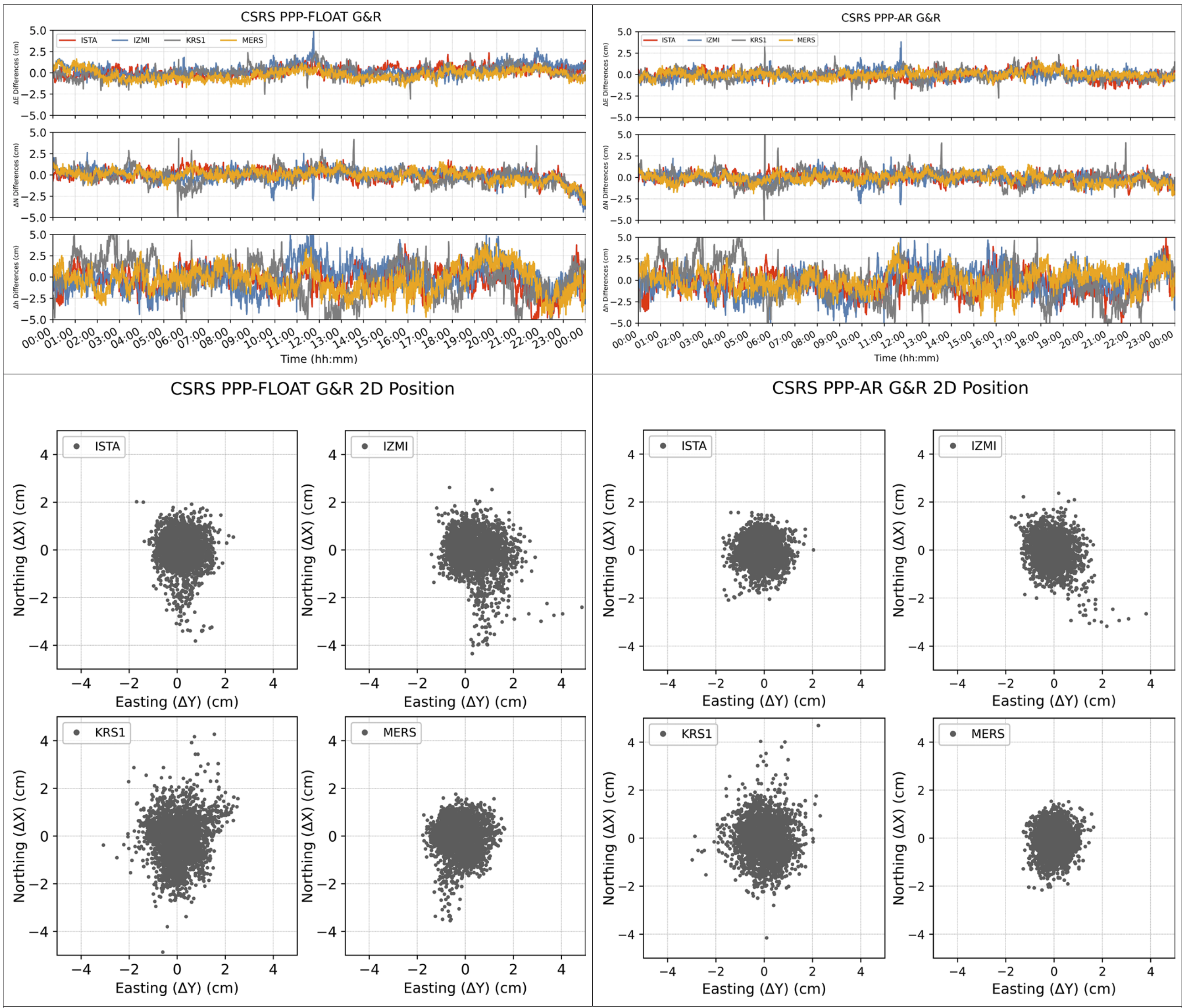

(b) GR combined solutions

Figure 7: Time series and scatter plots for Float/Fixed G-only (a) and GR (b) kinematic solutions.

12-hours with the GFZRNX open-source software. All RINEX data were processed as PPP-Float before the update and PPP-AR after the update using CSRS-PPP online service and compared with the known coordinates (ITRF) for each station.

In light of the results obtained from CSRS-PPP Float and Fixed solutions, it was obtained that the static PPP solutions of GPS and GPS&GLONASS data groups with different observation times provide accuracy in the order of cm to mm horizontally and vertically. With the addition of the GLONASS observations to the GPS observations, the horizontal and vertical accuracy increased in static PPP processes for both PPP-Float and PPP-AR and at all observation durations. Besides, as the observation duration increases, both static PPP-Float and static PPP-AR horizontal and vertical position accuracies also increased. The PPP-AR positioning technique has increased the horizontal and vertical position accuracy for both static and kinematic modes and for the whole satellite systems and observation durations, compared to the PPP-Float technique. According to the static and kinematic PPP-Float and PPP-AR solutions of the CSRS-PPP service, the highest accuracy was obtained by processing the 24-hourly GPS&GLONASS combination using the PPP-AR solution. Horizontal and vertical accuracies obtained from 24-hourly static PPP solutions are better than 5mm. In general, according to the static PPP solutions performed for 1-hour and 2-hour observation durations, the horizontal position and height accuracies are at the cm level. For observation durations from 4-hours to 24-hours, the accuracy values gradually increase to the level of millimeters. According to the horizontal and vertical accuracies obtained from static PPP-Float solutions performed for 1-hour and 2-hour observation durations, PPP-AR solutions increased the horizontal and vertical position accuracy by 50%.

As a result of this study, if the horizontal or vertical accuracy of 3 cm is desired using the PPP static technique,

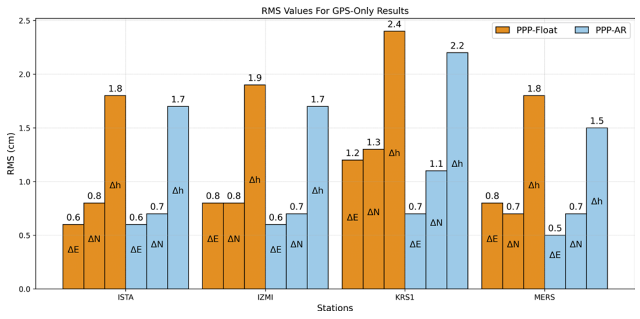

G-only solutions.

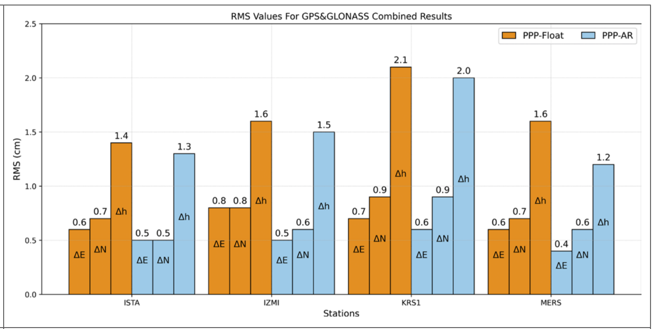

GR combined solutions.

Figure 8: Kinematic PPP-Float and PPP-AR RMS values.

1-hour of observation is sufficient. If below cm-level accuracy is required, the PPP-AR technique can be used with 1-hour of observations, depending on the data quality. The accuracies obtained from the 1-hour of observation can be increased by %50 for both PPP-Float and PPP-AR by doubling the observation duration (2-hours). Besides, 2-hours of static solutions using PPP-AR are sufficient for millimeter-level horizontal accuracy. If both horizontal and vertical accuracy is desired in mm-level in static mode, evaluating the minimum 4-hour observations using PPP-AR solution is sufficient.

Taking everything into consideration, it can be emphasized that the PPP-AR solution, which is included in the new version v3.45.0 of the CSRS-PPP service, significantly improves the horizontal position and height accuracies. With this upgrade, CSRS-PPP service has become a more alternative to classical relative positioning in terms of accuracy. In conclusion, the use of AR-supported PPP techniques in engineering studies that require more accuracy will increase, and the PPP-AR technique will be preferred more because it’s easy and economical to use.

Acknowledgement

The authors gratefully acknowledge the NRCan for CSRS-PPP service and the BKG for developing BNC software used in the study. The authors also thank the editor and anonymous reviewers, who make the article more powerful with their suggestions. The primary results of this study were presented at the IGD symposium in Mersin/Türkiye on November 25th-26th, 2020 (**Mutlu et al., 2020**).

7. References

Anderle, R. J. (1976): Point positioning concept using precise ephemeris. Satellite Doppler Positioning, 1, 47–75.

Atiz, O. F., and Kalaycı, I. (2021): Performance Assessment of PPP-AR Positioning and Zenith Total Delay Estimation with Modernized CSRS-PPP. Artificial Satellites, 56(2), 18-34. https://doi.org/10.2478/arsa-2021-0003

Bahadur, B., and Üstün, A. (2014): Internet tabanlı GNSS veri değerlendirme servisleri. Harita Dergisi, 152(2), 40–50.

Banville, S. (2020): CSRS-PPP Version 3: Tutorial. Last Update, 2020-08-25. https://webapp.csrs-scrs.nrcan-rncan.gc.ca/geod/tools-outils/sample_doc_filesV3/NRCan CSRS-PPP-v3_Tutorial EN.pdf (accessed 23rd May 2023).

Banville, S., Hassen, E., Lamothe, P., Farinaccio, J., Donahue, B., Mireault, Y., Goudarzi, M. A., Collins, P., Ghoddousi-Fard, R., and Kamali, O. (2021): Enabling ambiguity resolution in CSRS-PPP. Journal of the Institute of Navigation, 68, 433–451. https://doi.org/10.1002/navi.423

Bisnath, S., and Collins, P. (2012): Recent developments in precise point positioning. Geomatica, 66(2), 103–111. https://doi.org/10.5623/cig2012-023

Choy, S., Bisnath, S., and Rizos, C. (2017): Uncovering common misconceptions in GNSS Precise Point Positioning and its future prospect. GPS Solutions, 21, 13–22. https://doi.org/10.1007/s10291-016-0545-x

Collins, P. (2008): Isolating and estimating undifferenced GPS integer ambiguities. Proceedings of the 2008 National Technical Meeting of the Institute of Navigation, 720–732.

Collins, P., Bisnath, S., Lahaye, F., and Héroux, P. (2010): Undifferenced GPS ambiguity resolution using the decoupled clock model and ambiguity datum fixing. Navigation, 57(2), 123–135. https://doi.org/10.1002/j.2161-4296.2010.tb01772.x

Dawidowicz, K. (2020): Sub-hourly precise point positioning accuracy analysis–case study for selected ASG-EUPOS stations. Survey Review, 52(373), 341–351. https://doi.org/10.1080/00396265.2019.1579988

DeSanto, J. B., Chadwell, C. D., and Sandwell, D. T. (2019): Kinematic post-processing of ship navigation data using precise point positioning. The Journal of Navigation, 72(3), 795–804. https://doi.org/10.1017/S0373463318000887

Doucet, K., Herwig, M., Kipka, A., Kreikenbohm, P., Landau, H., Leandro, R., Moessmer, M., and Pagels, C. (2012): Introducing ambiguity resolution in web-hosted global multi-GNSS Precise point positioning with Trimble RTX-PP. Proceedings of the 25th International Technical Meeting of The Satellite Division of the Institute of Navigation (ION GNSS 2012), 1115–1125.

Elango, G. A., Sudha, G. F., and Francis, B. (2017): Weak signal acquisition enhancement in software GPS receivers – Pre-filtering combined post-correlation detection approach. Applied Computing and Informatics, 13(1). https://doi.org/10.1016/j.aci.2014.10.002

Erol, S., Alkan, R. M., Ozulu, I. M., and Ilçi, V. (2020): Performance analysis of real-time and post-mission kinematic precise point positioning in marine environments. Geodesy and Geodynamics, 11(6), 401–410. https://doi.org/10.1016/j.geog.2020.09.002

Facio, Y., and Berber, M. (2020): Subsidence is determined in the heart of the Central Valley using Post Processed Static and Precise Point Positioning techniques. Journal of Applied Geodesy, 14(1), 113–118. https://doi.org/10.1515/jag-2019-0043

Ge, M., Gendt, G., Rothacher, M., Shi, C., and Liu, J. (2008): Resolution of GPS carrier-phase ambiguities in precise point positioning (PPP) with daily observations. Journal of Geodesy, 82(7), 389. https://doi.org/10.1007/s00190-007-0187-4

Hatch, R. (1983): The synergism of GPS code and carrier measurements. International Geodetic Symposium on Satellite Doppler Positioning, 2, 1213–1231.

Héroux, P., and Kouba, J. (2001): GPS precise point positioning using IGS orbit products. Physics and Chemistry of the Earth, Part A: Solid Earth and Geodesy, 26(6–8), 573–578. https://doi.org/10.1016/S1464-1895(01)00103-X

Hofmann-Wellenhof, B., Lichtenegger, H., and Wasle, E. (2007): GNSS–Global Navigation Satellite Systems: GPS, GLONASS, Galileo, and more. Springer Science & Business Media.

Katsigianni, G., Loyer, S., and Perosanz, F. (2019): PPP and PPP-AR kinematic post-processed performance of GPS-Only, Galileo-Only and Multi-GNSS. Remote Sensing, 11(21), 2477. https://doi.org/10.3390/rs11212477

Kiliszek, D., Szołucha, M., and Kroszczyński, K. (2018): Accuracy of Precise Point Positioning (PPP) with the use of different International GNSS Service (IGS) products and stochastic modelling. Geodesy and Cartography, 67(2), 207–238. http://dx.doi.org/10.24425/gac.2018.125472

Klatt, C., and Johnson, P. (2017): Estimating benefits to Canada and the world: the Canadian Spatial Reference System Precise Point Positioning Service. Geomatica, 71(1), 37–44. https://doi.org/10.5623/cig2017-104

Laurichesse, D., Mercier, F., Berthias, J. P., Broca, P., and Cerri, L. (2009): Integer ambiguity resolution on undifferenced GPS phase measurements and its application to PPP and satellite precise orbit determination. Navigation, 56(2), 135–149. https://doi.org/10.1002/j.2161-4296.2009.tb01750.x

Loyer, S., Perosanz, F., Mercier, F., Capdeville, H., and Marty, J. C. (2012): Zero-difference GPS ambiguity resolution at CNES–CLS IGS Analysis Center. Journal of Geodesy, 86, 991–1003. https://doi.org/10.1007/s00190-012-0559-2

Melbourne, W. G. (1985): The case for ranging in GPS-based geodetic systems. Proceedings of the First International Symposium on Precise Positioning with the Global Positioning System, 373–386.

Mutlu, B., Erol, S., and Alkan, R. M. (2020): Comparison of Static PPP Performance of CSRS-PPP Float and Trimble RTX-PP Services. Intercontinental Geoinformation Days, 1, 173–176.

Nischan, T. (2016): GFZRNX-RINEX GNSS data conversion and manipulation toolbox (version 1.05). GFZ Data Services. https://doi.org/10.5880/GFZ.1.1.2016.002

Pırtı, A., Hoşbaş, R. G., and Yücel, M. A. (2023): Examination of the Earthquake (Samos Island) in Izmir (30.10.2020) by Using Cors-Tr GNSS Observations and InSAR Data. KSCE Journal of Civil Engineering, 27(1). https://doi.org/10.1007/s12205-022-0392-y

Shi, J. (2012): Precise Point Positioning integer ambiguity resolution with decoupled clocks. Doctoral thesis, University of Calgary, Calgary, Canada. https://doi.org/10.11575/PRISM/27397

Shi, J., and Gao, Y. (2014): A comparison of three PPP integer ambiguity resolution methods. GPS Solutions, 18, 519–528. https://doi.org/10.1007/s10291-013-0348-2

Topal, G. O., and Akpinar, B. (2022): High rate GNSS kinematic PPP method performance for monitoring the engineering structures: Shake table tests under different satellite configurations. Measurement: Journal of the International Measurement Confederation, 189. https://doi.org/10.1016/j.measurement.2021.110451

URL-1: Trimble Positioning Service. (2021): https://positioningservices.trimble.com/en/rtx (accessed 23rd May 2023).

URL-2: GeoED. (2019): CSRS-PPP-transitioning to a modernized positioning service in Canada. https://www.geoed.ca/product/csrs-ppp-transitioning-to-a-modernized-positioning-service-in-canada-product (accessed 23rd May 2023).

URL-3: BNC software. https://igs.bkg.bund.de/ntrip/bnc (accessed 23rd May 2023).

URL-4: The European Reference Frame (EUREF) Permanent Network (EPN). (2023). http://epncb.oma.be/_networkdata/data_quality/index.php?station=KRS100TUR (accessed 23rd May 2023).

Wessel, P., Luis, J. F., Uieda, L., Scharroo, R., Wobbe, F., Smith, W. H. F., and Tian, D. (2019): The generic mapping tools version 6. Geochemistry, Geophysics, Geosystems, 20(11), 5556–5564. https://doi.org/10.1029/2019GC008515

Wübbena, G. (1985): Software developments for geodetic positioning with GPS using TI 4100 code and carrier measurements. Proceedings 1st International Symposium on Precise Positioning with the Global Positioning System, 403–412.

Xiao, G. (2022): Multi-frequency and multi-GNSS PPP phase bias estimation and ambiguity resolution. KIT Scientific Publishing. https://doi.org/10.5445/KSP/1000124935

Xu, G., and Xu, Y. (2007): GPS Observation Equations and Equivalence Properties. In: GPS. Springer -Verlag Berlin Heidelberg. https://doi.org/10.1007/978-3-662-50367-6

Zumberge, J. F., Heflin, M. B., Jefferson, D. C., Watkins, M. M., and Webb, F. H. (1997): Precise point positioning for the efficient and robust analysis of GPS data from large networks. Journal of Geophysical Research: Solid Earth, 102(B3), 5005–5017. https://doi.org/10.1029/96JB03860

SAŽETAK

Analiza performansi statičkoga i kinematičkoga PPP-AR servisa temeljene na internetu pri naknadnoj obradi

Korištenje tehnike preciznoga pozicioniranja (PPP) postalo je vrlo povoljno s razvojem tehnologije GNSS pozicioniranja. Moguće je dobiti vrlo precizne informacije o položaju bez potrebe za podatcima referentne stanice korištenjem PPP tehnike. Međutim, postoje različiti čimbenici koji utječu na točnost rješenja PPP-a, uključujući vrstu rješenja dvosmislenosti početne faze koja može biti fiksna ili pomična, atmosferske učinke, duljinu promatranja, korištene satelitske sustave i korištene precizne proizvode. Usluga Canadian Spatial Reference System-Precise Point Positioning (CSRS-PPP) jedna od internetskih PPP usluga, ažurirana je 20. listopada 2020. i nadograđena na verziju 3, koja podržava rješenje s fiksnom dvosmislenošću (PPP-AR). Do sada je usluga nudila rješenje Ambiguity-Float (PPP-Float). U ovoj studiji cilj je istražiti učinak korištenja različitih satelitskih sustava (GPS, GPS&GLONASS), duljine vremena promatranja, statičkih/kinematičkih načina obrade i tipova rješenja dvosmislenosti početne faze na točnost PPP-a. Dnevni podatci motrenja ANKR, ISTA, IZMI, MERS i KRS1 IGS GNSS postaja koje se nalaze unutar granica Turske podijeljeni u različite podsesije (1-satni, 2-satni, 4-satni, 8-satni i 12-satni) obrađeni su korištenjem CSRS-PPP internetske usluge kao PPP-Float prije ažuriranja i PPP-AR nakon ažuriranja. Kao rezultat usporedbe, kombinirana upotreba GPS i GLONASS satelitskih sustava umjesto korištenja samih GPS satelita povećala je horizontalnu i vertikalnu točnost u statičkim/kinematičkim PPP-Float i PPP-AR rješenjima. Uzimajući u obzir statička rješenja, horizontalna i vertikalna točnost položaja povećavaju se kako se povećava vrijeme promatranja u objema metodama rješenja višeznačnosti koristeći se različitim konstelacijama. U slučaju usporedbe metoda rješavanja višeznačnosti utvrđeno je da PPP-AR pristup nudi veću točnost od PPP-Float u svim slučajevima rješenja.

Ključne riječi:
GPS, GLONASS, PPP-AR, PPP-Float, CSRS-PPP

Authors’ contribution

Bilal Mutlu: Methodology, investigation, validation, visualization, software. **Serdar Erol:** Conceptualization, supervision, validation, analysis, writing-reviewing, and editing. **Reha Metin Alkan:** Conceptualization, supervision, validation, analysis, writing-reviewing, and editing.